


Review Article

# Development of a standard phantom for diffusion-weighted magnetic resonance imaging quality control studies: A review

Eric Naab MANSON <sup>1,ABCDEF,\*</sup>, Abdul Nashirudeen MUMUNI<sup>1,ACEF</sup>, Issahaku SHIRAZU<sup>2,ACEF</sup>, Francis HASFORD<sup>3,ACEF</sup>, Stephen INKOOM<sup>2,DEF</sup>, Edem SOSU<sup>2,CEF</sup>, Mark Pokoo AIKINS<sup>2,ABDF</sup>, Gedel Ahmed MOHAMMED<sup>3,ABCF</sup>

<sup>1</sup>Department of Medical Imaging, University for Development Studies, Ghana

<sup>2</sup>Radiological and Medical Sciences Research Institute, Ghana Atomic Energy Commission, Ghana

<sup>3</sup>Medical Physics, University of Ghana, Ghana

\*Corresponding author: Eric Naab Manson; mansonericnaab@yahoo.com

(received 16 April 2022; revised 4 July, 8 August and 19 September 2022; accepted 3 October 2022)

## Abstract

Various materials and compounds have been used in the design of diffusion-weighted magnetic resonance imaging (DW-MRI) phantoms to mimic biological tissue properties, including diffusion. This review thus provides an overview of the preparations of the various DW-MRI phantoms available in relation to the limitations and strengths of materials/solutions used to fill them. The narrative review conducted from relevant databases shows that synthesizing all relevant compounds from individual liquids, gels, and solutions based on their identified strengths could contribute to the development of a novel multifunctional DW-MRI phantom. The proposed multifunctional material at varied concentrations, when filled into a multi-compartment Perspex container of cylindrical or spherical geometry, could serve as a standard DW-MRI phantom. The standard multifunctional phantom could potentially provide DW-MRI quality control test parameters in one study session.

**Keywords:** diffusion-weighted magnetic resonance imaging; apparent diffusion coefficient; phantom; quality control.

## Introduction

Diffusion-weighted imaging (DWI) offers valuable information that improves the sensitivity of MRI as a diagnostic tool, reduces the range of possible diagnoses, offers prognostic data, helps with treatment planning, and assesses therapy response.<sup>1</sup> Diffusion-weighted magnetic resonance imaging (DW-MRI) has proven to be a promising, reliable and dependable technique in the early detection of pathologies such as stroke. For example, ischemic injury can easily be visualized in diffusion-weighted images of early acute stroke, through the calculated apparent diffusion coefficient (ADC) value before any changes can be observed in  $T_1$ - and  $T_2$ - weighted MRI. Early detection of such injury can significantly influence the treatment and potential recovery of patients diagnosed with stroke.<sup>2</sup> DWI technique quantifies the amount of water molecules diffusion using a monoexponential model. The technique is based on the generation of contrast resulting from the diffusion of randomly moving water molecules in tissue. In order to record the diffusion effect in MRI, two rectangular gradient fields of equal amplitude and duration are applied before and after the 180° refocusing radiofrequency pulse in the standard spin-echo pulse

sequence. The amounts of diffusion, measured as the b-value, and nuclear magnetic resonance signal attenuation  $[S]$  determine the measured apparent diffusion coefficient (ADC) of water molecules in biological tissues<sup>3</sup> given by **Equation 1**.

$$S = S_0 e^{-bADC} \quad \text{Eq. 1}$$

Where,  $S_0$  is the MRI signal obtained without diffusion (i.e.,  $b = 0 \text{ s/mm}^2$ ),  $S$  is the MRI signal obtained after the diffusion gradients have been applied,  $b$  is the strength of diffusion (in  $\text{s/mm}^2$ ) and ADC is the monoexponential apparent diffusion coefficient of water in an image voxel.

The total ADC in the voxel is also calculated (given in **Equation 2**) by averaging the fast and slow diffusion coefficients in tissues where there is biexponential decay of DW signals, such as the brain or pancreas, where both slow diffusion coefficient and fast diffusion coefficient are experienced within the extracellular and intracellular spaces of the tissue.<sup>4</sup>

$$\frac{S_y}{S_0} = (1 - f)e^{-bD} + fe^{-bD^*} \quad \text{Eq. 2}$$

Where  $b$  is the strength of diffusion (measured in  $\text{s/mm}^2$ ),  $S_0$  is the MRI signal obtained before diffusion ( $b = 0 \text{ s/mm}^2$ ),  $S_y$  is the

MRI signal obtained after diffusion gradients have been applied,  $D$  is the diffusion coefficient in the slow compartment,  $D^*$  is the diffusion coefficient in the fast compartment, and  $f$  is the flowing fraction.

In certain regions of biological tissues, the presence of microstructures affects the free flow of water molecules, which results in non-Gaussian behavior. In such situations, the Kurtosis model and the stretched model are frequently used to estimate tissue diffusion deviation from the Gaussian model.<sup>5-7</sup>

The echo-planar sequence is the magnetic resonance imaging technique that can provide adequate information about the diffusion of water molecules in biological tissue through the apparent diffusion coefficient.<sup>8</sup> The displacement of water molecules measured in biological tissues using the pulse gradient spin-echo nuclear magnetic resonance technique is in the range of 1.5 – 15  $\mu\text{m}$ .<sup>9</sup> The apparent diffusion coefficient is heavily influenced in intracellular regions by the presence of neurofilaments and microtubules than in extracellular regions, which contain glial cells. As a result, ADC (i.e.,  $0.75 \times 10^{-9} \text{ m}^2/\text{s}$ ) is lower in intracellular regions as compared to ADC (i.e.,  $2.0 \times 10^{-9} \text{ m}^2/\text{s}$ ) in extracellular regions.<sup>8</sup>

DWI phantoms enable the evaluation of fit model-specific bias and uncertainty for quantitative diffusion parameters, which helps to distinguish noise-induced errors from tissue properties and direct the development of a quantitative DWI methodology.<sup>10</sup> Phantoms used for DW-MRI quality control tests often have higher diffusivity properties, relatively low  $T_1/T_2$  contrast, and a limited range of molecular diffusivity within the available volume of the phantom. These conditions differ significantly from *in vivo* conditions.<sup>11</sup> The random motion of molecular compounds in biological tissues can be described as either isotropic or anisotropic. In isotropic diffusion, the molecules diffuse freely in all directions without restriction. However, in anisotropic diffusion, molecular motion is asymmetric since motion occurs along a specific direction.

The geometry of isotropic phantoms is either spherical, cylindrical or tubes filled with gels or liquids that exhibit similar relaxation and/or diffusion properties as the water molecules in biological tissues. Examples of such liquids and gels include alkanes, agarose, and polyethylene glycol (PEG). Polysaccharide-based gels such as carrageenan have also been used for isotropic phantoms.<sup>12</sup> Polysaccharides have similar properties to human tissues, and are thus commonly used in MRI phantoms. They are simple sugar monomers with structural elements of cell walls containing intracellular spaces and connective tissue. Each monomer unit is made up of one to six groups of C-OH which allow for hydrogen bonding in hydrated gels. The bonding mechanism also permits the water proton  $T_1$  and  $T_2$  relaxation properties to be altered.<sup>13</sup> Other gels include sodium alginate, xanthan gum, FAVOR-PAC-300, PNC-,

Carbomer-980, and Carbopol-974P. When gels are used for phantoms, their images are of better quality (with fewer distortions) as compared to images obtained with phantoms made of liquids due to the reduction of the macroscopic flow effect.<sup>12</sup> Anisotropic phantoms are more suitable and useful for diffusion tensor imaging than for diffusion-weighted imaging. This is owing to anisotropic phantoms' increased stability, which lowers imaging artifacts brought on by a drop in the macroscopic water flux when they are constructed from layers of an isotropic gel based on agar.<sup>14</sup>

This review provides an overview of the benefits and drawbacks of several diffusion-weighted magnetic resonance imaging (DW-MRI) phantom construction methods towards creating a standard DW-MRI phantom for carrying out quality control testing.

## Methods

Using relevant online databases, such as Scopus, PubMed/Medline, and Google Scholar, a narrative search on general diffusion-weighted MRI phantoms was undertaken from 1974 to 2020. "Diffusion-weighted," "MRI," and "phantom" were among the search terms. **Table 1** shows a summary of some data extraction from relevant articles.

## Construction of DW-MRI phantoms

Ideally, DW-MRI phantoms should be capable of differentiating between ADC values of different tissues. For example, the ADC for both normal liver and pancreas ranges from 80 to  $440 \times 10^{-5} \text{ mm}^2 \text{ s}^{-1}$ , while for a pathological liver and pancreas, the ADC ranges from 104 to  $381 \times 10^{-5} \text{ mm}^2 \text{ s}^{-1}$ , and 176 to  $396 \times 10^{-5} \text{ mm}^2 \text{ s}^{-1}$  respectively.<sup>15</sup> Improved anisotropic phantoms are more appropriate for validating ADC measurements. However, developments of tissue-mimicking phantoms for precise and accurate ADC measurement of DW-MRI protocols are limited by the complex cellular environments of living tissues.<sup>13</sup> To accurately develop protocols for *in vivo* DW-MRI studies, there is the need to use phantoms that are purposefully designed and constructed to meet the standards of both geometry and tissue-mimicking contents for DW-MRI. Some proposed requirements include isotropic test tube phantoms filled with liquid, fiber phantoms to mimic axonal tracts or cardiac muscles, capillary phantoms with diffusion properties and relaxation times similar to biological tissues, green asparagus water phantoms, animal tissues that simulate axons of pigs or mice, and computational phantoms.<sup>12</sup> **Table 2** shows some DW phantoms, the components used for their construction, and examples of some tissues they mimic.

**Table 1. Summary of data extracted from relevant articles (continued on the next page)**

Author	Year	Journal/Publisher	Country	Aim	Results	Ref.
Bammer	2003	European Journal of Radiology	USA	To discuss the fundamentals of DWI and Diffusion Tensor Imaging.	In-vivo diffusion coefficients could help researchers better understand normal and pathological physiology in the human body. To verify DWI's potential to diagnose illnesses, more clinical trials are needed.	3
Le Bihan	2015	PLOS Biology	France	To provide a deeper understanding of DWI mechanisms	The use of DW-MRI in the diagnosis of brain disease, and neurological problems, and the detection and management of cancer lesions are particularly beneficial. Diffusion allows for high field strength operation, biological molecule interaction, and cell metabolism interaction.	24
Posnansky & Shah	2008	Journal of Biological Physics	Germany	To investigate the impact of a wide variety of microstructural and compositional characteristics on the apparent diffusion coefficient using a geometrical model	The apparent diffusion coefficient is strongly influenced by the ratio of the microscopic diffusion coefficients of the constituent phases, their concentrations, and the permeability of the cells	8
Cooper et al.	1974	Biophysical Journal	USA	To investigate restricted diffusion in biological systems	The presence of bound or trapped water in tissues at short diffusion times is evidenced by diffusivities in tissues. Cell membranes and mitochondria are responsible for limitations in red blood cells and rat liver, respectively.	9
Laubach et al.	1998	Journal of Magnetic Resonance Imaging	USA	To develop MRI diffusion phantom that mimics acute stroke and normal gray matter (GM) using agar gel and sucrose solutions	The ADC between agar gels and sucrose solutions was similar to the human ADC between GM and acute stroke. The partial volume effect increased with slice thickness, resulting in percentage volumetric error estimations based on the DW EPI of sucrose solution between measured and real volumes of acute stroke compartments.	2
Kato et al.	2005	International Journal of Medical Physics, Research and Practice	Japan	To develop and evaluate the performance of a NaCl CAG phantom using carrageenan gel, NaCl, agarose, NaN <sub>3</sub> , GdCl <sub>3</sub> , and water	The phantom has sufficient strength to represent the torso and could be useful for electrical conductivity tests, such as those used in MRI and hyperthermia research.	11
Souza et al.	2017	Research on Biomedical Engineering	Brazil	To explore the proposed DWI and DTI phantoms, the issues they pose, and future prospects for DWI and DTI QC	Anisotropic and isotropic diffusion phantoms could be constructed using Dyneema and synthetic polymer gels with $T_1$ , $T_2$ , and ADC values similar to those found in biological tissues.	12
Kivrak et al.	2013	Diagnostic and Interventional Radiology	Turkey	Using a custom-made phantom solution consisting of distilled water, NaCl, and shampoo to compare ADC values of different MRI scanners.	Various MRI systems used for DW-MRI may have different ADC values. When employing DW-MRI in a clinical context, the type of MRI scanner should be considered.	13
Groch et al.	1991	Magnetic Resonance Imaging	USA	To construct an MRI tissue equivalent lesion phantom using a polysaccharide material TX 150 gel	Using 2-2-diphenyl-1-picrylhydrazyl as a $T_2$ modifier and metal phthalocyanines as a $T_1$ modifier, a septumless lesion phantom with varying $T_2$ and $T_1$ relaxation properties could be created.	16
Mazzara et al.	1996	Magnetic Resonance Imaging	USA	To create a tissue equivalent MRI phantom with polysaccharide material, TX-151, water, NaCl, and Al powder	Gd-DTPA can be used as a $T_1$ and $T_2$ modifier to construct phantoms with a wide range of relaxation times to resemble various human tissues and organs. The TX-151 gel, when combined with additional materials like fat and silicone implants, could be used to construct a human breast phantom for MRI research	17
Vassiliou et al.	2016	Journal of Cardiovascular Magnetic Resonance	UK	To test the stability of nickel-based phantoms utilized for myocardial $T_1$ /ECV mapping	All native and post-gadolinium $T_1$ values showed small relative changes up to 9.0 %, while phantom ECV showed a 2.2 percent maximal absolute change. The native and post-gadolinium $T_2$ readings, on the other hand, remained steady over time with <2 % variation. To determine index for rectification in the event of a scanner upgrade or alteration, monthly re-scanning is recommended against phantom drift.	18

**Table 1. Summary of data extracted from relevant articles (continued from the previous page)**

Author	Year	Journal/Publisher	Country	Aim	Results	Ref.
Lavdas et al.	2013	Journal of Magnetic Resonance Imaging	UK	To create tissue-equivalent diffusivity materials and a spherical diffusion phantom to mimic biological tissues using Nickel-doped agarose/sucrose gels	$T_1$ relaxation times of the gels are determined by sucrose concentrations, while $T_2$ are determined by agarose concentration. ADC was affected by only sucrose concentration. To achieve a low ADC value of the gel, $T_1$ could be regulated with only sucrose concentration without affecting $T_2$ relaxation time	19
Captur et al.	2016	Journal of Cardiovascular Magnetic Resonance	UK	To develop and check the stability of an agarose gel-based phantom using a nickel chloride modifier for quality assurance purposes	$T_1$ ( $0.64 \pm 0.45\%$ ) and $T_2$ ( $0.49 \pm 0.34\%$ ) values at 1.5 T and 3 T respectively, assessed in T <sub>1</sub> MES had 1% or less variance between repeat scans, demonstrating high short-term repeatability	20
Kim et al.	2019	PLOS One	South Korea	To show how a spherical phantom with spherical inner compartments can be constructed using gelatin sphere doped with paramagnetic contrast agents	The overall geometry of the phantom could eliminate bulk background phase caused by the air-phantom boundary. The spherical geometry of the phantom could suppress inhomogeneous spin dephasing and produce a homogeneous $B_0$ field inside the inclusions spheres, with an effective transverse relaxation rate nearly equal to the transverse relaxation rate.	21
Hara et al.	2014	Oncology Letters	Japan	To create a phantom for 3T MRI that mimics ADC values of normal and tumor tissues using different sucrose concentrations	The ADC values measured ranged from $0.33$ to $3.02 \times 10^3$ mm <sup>2</sup> /sec, covering the range of ADC values of the human body measured clinically by 3T MRI.	22
Kalaitzakis et al.	2020	Physica Medica	Greece	To create a new DWI-MRI phantom and compare ADC measurements using sucrose concentrations and polyacrylamide gels	In comparison to sucrose solutions, polyacrylamide gels have a smaller coefficient of variation and therefore could be a superior way to simulate ADC values.	15
Gatidis et al.	2014	Magnetic Resonance in Medicine	Germany	To create a diffusion-weighted imaging (DWI) phantom with predetermined apparent diffusion coefficients (ADC) and $T_2$ relaxation times using polyethylene glycol (PEG) solutions	Increased PEG concentrations resulted in a significant reduction in diffusivity and minor changes in $T_2$ relaxation times. ADC values and $T_2$ relaxation times could be adjusted to predefined values by the addition of gadobutrol to the PEG solutions	23
Khasawneh et al.	2020	Biomedical Reports	Japan	To assess if phantoms made of polyethylene glycol (PEG) could be utilized as standard phantoms for magnetic resonance imaging (MRI)	The ADC value drops as the PEG concentration rises. Within a limited range of clinically reported diffusion kurtosis imaging (DKI) values, the PEG phantom was found to imitate restricted diffusion. The PEG phantom is safer than the ADC standard phantoms - gelatinous substances like agar, agarose, and polyacrylamide, as well as liquid solution materials like ethanol, acetone, Gd-DTPA solution, and cupric sulfate solution - that have been previously described.	25
Fieremans & Lee	2018	Neuroimage	USA	To provide an overview of how to create, implement, or choose the proper phantom for microstructure mapping.	Understanding all parameters affecting microstructural MR contrasts, both experimentally and in simulations, could be crucial to comprehending phantom behavior and building a universal multimodal microstructural phantom.	28
Yoshida et al.	2016	The British Journal of Radiology	Japan	To evaluate image quality and ADC values of single-shot turbo spin echo (TSE) DW images using a parallel imaging (PI) technique	Due to image noise and artefacts associated with the PI approach, TSE-DWI images had lower SNRs, impairing ADC measurements.	29

**Table 2. DW phantoms components and tissues they mimic**

Types of DWI phantom	Components	Geometry	Examples of tissues
Polysaccharide gel phantom	Polysaccharide powder, distilled water, de-gassed water, paramagnetic metal complex solution, gelling solution, propyl paraben material, phthalocyanine dye, picrylhydrazyl	cylindrical	breast
Nickel chloride phantoms	Polysaccharide material, water, NaCl, Al powder and Gd-DTPA Nickel (II) chloride hexahydrate (NiCl <sub>2</sub> ·6H <sub>2</sub> O) stock solutions, deionized water, distilled water, agarose powder Nickel (II) chloride hexahydrate, agarose, sucrose, sodium chloride solution, deionized water, diazolidinyl urea, paramagnetically doped agarose or carrageenan gels	cylindrical spherical	myocardial tissues and native blood
Acrylic perspex phantom	Acrylic perspex spheres, aqueous solution of gelatin powder, nickel, agarose, and sucrose concentrations	spherical	cyst, fat
Sucrose phantom	Sucrose, NaN <sub>3</sub> antiseptic, distilled water	cylindrical	normal tissues (e.g., brain, muscle, prostate, breast) lesions (e.g., brain, thyroid gland, pancreas, uterine cervix, ovary, prostate)
Polyacrylamide phantom	Acrylamide solution containing acrylamide:bisacrylamide, deionized water, ammonium persulfate solution, N,N,N',N'-tetramethylethylenediamine	cylindrical	whole range of human physiologic and pathologic soft tissues
Agarose phantom	Agarose gel, distilled water, acrylamide:bisacrylamide, ammonium persulfate solution, N,N,N',N'-tetramethylethylenediamine	cylindrical	whole range of human physiologic and pathologic soft tissues
Polyethylene glycol (PEG) phantom	PEG and gadobutrol compounds, deionized water, agarose gel PEG diffusion modifier, NaN <sub>3</sub> antiseptic, distilled water, NaCl	cylindrical	grade II glioma, squamous cell carcinoma, olfactory neuroblastoma, brain lymphoma
CMRI diffusion phantom	Polyvinylpyrrolidone (PVP) powder, water, distilled H <sub>2</sub> O	spherical	brain

### Polysaccharide/water gel phantom

Different samples of polysaccharide/water gel phantoms have been prepared using polysaccharide powder, distilled water, de-gassed water, paramagnetic metal complex solution, gelling solution,  $T_2$  modifier, and propylparaben material. These samples are prepared to examine the effect of paramagnetic oxygen and the influence of the propylparaben material on  $T_1$  and  $T_2$  values of the gels, as well as their long-term stability. Appropriate samples of these components are obtained by weighing them on a scale, after which they are mixed and stirred together until a partly solid mixture is produced. With the aid of a syringe, each prepared mixture is transferred into a nuclear magnetic resonance (NMR) tube, marked and sealed with a paraffin polymer wax. Phthalocyanine dye is used as  $T_1$  modifier due to its ability to electrostatically bind to the organic substrates used for the gel phantom. A stable water-insoluble free-radical such as 2-2-diphenyl-1 picrylhydrazyl is used as  $T_2$  modifier in the phantom.<sup>16</sup> In some circumstances, the polysaccharide material/water is used together with sodium chloride, Al powder, and Gd-DTPA to develop the phantom. The Gd-DTPA is used as a  $T_1$  and/or  $T_2$  modifier, while the Al powder aids the phantoms to produce a desirable range of relaxation times similar to human tissues by reducing high  $T_2$  values.<sup>17</sup>

The concentration of the gel, size of the modifier, temperature of the gelling solution, and gelling retardant can influence image uniformity. To access image uniformity, the polysaccharide water gel must be prepared such that it is homogeneous. The

spatial confinement of the modifying agents can be evaluated using a two-compartment cylinder filled with polysaccharide water gel phantom of different modifier solutions. For example, by measuring the diameters of both inner and outer cylinders, the interface between the inner and outer cylinders can be determined quantitatively using regions of interest (ROIs) on different image slices. In addition, by measuring the variations in signal intensity, the diffusion characteristics of the phantom can be assessed.<sup>16</sup>

### Nickel chloride (NiCl<sub>2</sub>) phantoms

Quality control MRI phantom for evaluation of myocardial  $T_1$  and extracellular volume fraction (ECV) mapping has also been developed using Nickel chloride (NiCl<sub>2</sub>) agarose gel. The phantom is formulated to mimic specific  $T_1$  and  $T_2$  myocardial and native blood values. In its construction, nickel-doped gels are carefully selected to vary proton  $T_1$  rates while  $T_2$  rates are determined by agarose concentrations.

To create the phantom, nickel (II) chloride hexahydrate (NiCl<sub>2</sub>·6H<sub>2</sub>O) stock solutions of different concentrations are made and frozen in a refrigerator. A suitable quantity of NiCl<sub>2</sub>·6H<sub>2</sub>O is washed with deionized water into a flask and intermittently filled with distilled water and stirred until the desired volume of the final stock solution is reached at room temperature. To formulate a required phantom with specific  $T_1$  and  $T_2$  values, a prescribed weight of agarose powder is mixed with a specific volume of the stock solution and poured into a

conical flask (of volume  $\geq 150$  ml). Distilled water is added and stirred to titrate up to the 150 ml volume. To ensure that the agarose is completely dissolved so that the desired  $T_1$  and  $T_2$  values are obtained, the  $\text{NiCl}_2$  agarose gel mixture is further heated in a microwave oven to approximately the boiling point equivalent to the  $T_1$  and  $T_2$  values of myocardial tissue. To ensure minimal vessel permeability and to avoid potential contact with air, the heated final  $\text{NiCl}_2$  agarose gel mixture is transferred carefully into a smaller narrow neck glass bottle (of volume  $\approx 60$  ml) and cooled.<sup>18</sup>

During the formulation process, it is important to ensure that no air bubbles are present in the gel, as the presence of air bubbles could be trapped in the solidified gel which could potentially increase distortions in the main static magnetic field ( $B_0$ ), cause cracks on the narrow neck bottle during cooling of the phantom and introduce inaccuracies in drawing of ROI to obtain intensity values for  $T_1$  and ADC calculations.<sup>18</sup>

Alternatively, Nickel (II) nitrate hexahydrate has been used to develop a spherical diffusion phantom that mimics biological tissues. Such phantoms have been formulated from a mixture of agarose, sucrose, and sodium chloride solutions. The solutions are mixed together with deionized water, stirred, and heated in a microwave to dissolve the agarose until a clear solution is formed. The hot mixture is continuously stirred until the temperature drops to below  $80^\circ\text{C}$ . Nickel (II) nitrate hexahydrate and 6 g/L of Diazolidinyl urea are added. To ensure that all the components are completely dissolved, the resulting mixture is further stirred until the temperature reduces to less than  $60^\circ\text{C}$ . The whole mixture is transferred into centrifuge tubes and allowed to settle at room temperature. The purpose of adding sodium chloride and Diazolidinyl urea to the gel is to mimic the electrical conductivity of biological tissues and to preserve the tissue-mimicking gels, respectively. The gels are prepared in three different ways; (1) the sucrose and agarose concentrations are kept constant, while the nickel concentration is varied. (2) the nickel and agarose concentrations are kept constant, while the sucrose concentration is varied. (3) the sucrose and nickel concentrations are kept constant while the agarose concentration is varied. The reason for these variations is to make it possible to independently measure the relaxation and diffusion properties of the various gel concentrations.<sup>19</sup>

Also, the initial formulation of the nickel chloride phantom involves designing several prototypes, such that the resulting  $T_1$  and  $T_2$  values are within a reasonable range, while mimicking native blood and myocardium tissues. Several test mixtures containing varying concentrations of  $\text{NiCl}_2$ , water, and agarose were prepared by dissolving them at  $95^\circ\text{C}$  in 50 ml test tubes in order to characterize the relationship between  $T_1$ ,  $T_2$ , agarose, and  $\text{NiCl}_2$ . The prepared samples were transferred into NMR tubes and analyzed with a Bruker minispec mq60 relaxometer after allowing them to settle. Results obtained from the analysis are fitted exponentially to determine  $T_1$  and  $T_2$  relaxation times. Finally,  $T_1$  and  $T_2$  values are modeled to determine the

relationship between the relaxation rates, agarose, and  $\text{NiCl}_2$  concentrations. Using the modeled equation, for any given concentrations of agarose and  $\text{NiCl}_2$ , the desired combinations of  $T_2$  and  $T_1$  values could be calculated for 1.5 T and 3 T phantoms.<sup>20</sup>

### Gel-filled acrylic Perspex spherical phantom

This consists of acrylic Perspex spheres of different dimensions filled with different concentrations of gels to mimic free diffusivity and diffusion properties of healthy tissues and benign lesions (or cysts). The inclusion of smaller compartments in the lower part of the phantom is to provide a means for the assessment of certain important properties of EPI DW-MRI such as fat suppression techniques and artifacts resulting from susceptibility effects. The concentrations of the gels in the various compartments are determined through measurements of their relaxation and diffusion properties while in the centrifuge tubes.<sup>19</sup> Alternative acrylic gel phantom compartments are made from an aqueous solution of gelatin powder, where diffusion of water molecules between the boundaries of the gel is reduced by mixing the gel solution with buffered formalin solution.<sup>21</sup>

### Sucrose phantom

This has been purposely designed for the calculation and comparison of ADC measurement in the ranges of normal and tumor tissues. It contains a mixture of sucrose,  $\text{NaN}_3$  antiseptic, and distilled water which is heated and stirred to completely dissolve the contents. The resulting solution is cooled, from which different concentrations are produced by varying the levels of both sucrose and  $\text{NaN}_3$ . The different concentration levels of the final solution represent normal (brain, muscle, and prostate) tissues and lesions (brain, thyroid gland, pancreas, uterine cervix, ovary, prostate, and transition zone) with distinct ADC values. The ADC represents specific characteristics of tissues. The solution is poured into different cylindrical containers.<sup>15,22</sup>

The case container (containing different sucrose phantoms) is fixed in a heating box made of Styrofoam and heated in the bore of the MRI scanner at different temperatures (within the body temperature range at  $1^\circ\text{C}$  interval) with the aid of a temperature-regulated water bath. DW images are acquired of at least four sucrose phantoms, each from  $28$  to  $39^\circ\text{C}$ , using echo-planar imaging techniques. Finally, ADC values are calculated from **Equation 1** using the signal intensity values obtained from a specific region of interest (ROI) in each of the sucrose phantom DW images.<sup>22</sup>

### Polyethylene glycol (PEG) phantom

Polyethylene glycol (PEG) is another class of compounds that has been used successfully to create a DW-MRI phantom. To make the phantom, PEG and gadobutrol compounds are dissolved in a graduated cylindrical plastic tube using deionized

water to produce different concentrations of PEG solution.<sup>23</sup> At a temperature of 37°C, the self-diffusion coefficient of free water is approximately  $3.0 \times 10^{-9} \text{ m}^2/\text{s}$ .<sup>24</sup> Since a DW image is  $T_2$  weighted, a specific average molar mass of the PEG compound is used for adjustment of water diffusivity while gadobutrol (a gadolinium-based compound) is used to adjust  $T_2$  relaxation times. By fitting the values of the resulting concentrations of both PEG and gadobutrol solution with defined ADC values of specific tissues using monoexponential and bi-exponential models, the behaviors of  $T_2$  relaxation times and water diffusivity can be predicted respectively.<sup>23</sup> Results obtained from the fits are used to estimate the exact concentrations of both PEG and gadobutrol solution required to develop the final phantoms. To prepare the final phantoms, different concentrations of PEG and gadobutrol solution are prepared in plastic tubes such that possible combinations of selected ADC and  $T_2$  relaxation values are similar to specific biological tissues. Each of the phantoms in the plastic tubes is placed in a plastic box and covered with a 2% agarose gel.<sup>23</sup>

Alternatively, PEG diffusion modifier,  $\text{NaN}_3$  antiseptic, and distilled water have also been used to create a PEG phantom. A mixture of diffusion modifier and the antiseptic is heated and later diluted using distilled water to achieve different concentrations with 0.03% w/w  $\text{NaN}_3$ . Empirical formulae are used to calculate the concentrations of the PEG such that they correspond to arbitrary ADC values. The resulting solutions are transferred into microcuvettes, from which each microcuvette is installed in a phantom case containing 0.9% NaCl and used as PEG phantoms. With the aid of a heating device connected to a circulating thermostat chamber, the temperature of the phantom is set to the body temperature of about 37°C. As the concentration of the PEG phantom increases, its ADC values decrease.<sup>25</sup>

### Polyacrylamide phantom

In the presence of a catalyst and a polymerization reaction initiator, a mixture of acrylamide and bisacrylamide (a cross-linker) is chemically polymerized to create polyacrylamide gels phantoms<sup>26-27</sup> that can mimic the ADC values of biological tissues. Higher polyacrylamide gel monomer concentrations (between 60 and 90%) are advised to evaluate lower ADC values. Similar to this, lower polyacrylamide gel monomer concentrations (20–40%) are required for larger ADC readings.<sup>15</sup> To replicate lower ADC values of biological tissues, different test tubes are filled to about two-thirds with lower monomer concentrations of polyacrylamide gel or in co-monomer ratios of 1/20, 1/30, and 1/40. This is then followed by the addition of tetramethylethylenediamine and ammonium persulfate to catalyze the polymerization of acrylamide. The final mixture is then placed in a plastic holder embedded in a water tank at a room temperature of  $22 \pm 1^\circ\text{C}$ .<sup>15</sup>

### Discussion

The microstructural properties of the phantom material can affect the NMR properties of the liquids, gels, or solutions that fill them. This may lead to restricted diffusivity, and cause local field inhomogeneities due to magnetic susceptibility effects. Quality control phantoms can be made to completely mimic MR properties. For example, effects such as relaxation, diffusion, and susceptibility properties of brain phantoms can be created by doping water or gel such that its microstructural parameters mimic the tissues in the human brain. Ideally, the materials used in the preparation of DW-MRI phantoms should be accessible, cost-effective, stable, independent of  $T_2$  relaxation times, non-toxic, and must have ADC similar to biological tissues.<sup>28</sup>

The average distance between biological fibers and average displacement of the water molecule is between 12 – 18  $\mu\text{m}$  and 8 – 35  $\mu\text{m}$  respectively. To obtain a uniform attenuation in biological tissues and the desired MRI signal, it is critical to ensure that, diffusion-weighted MRI phantoms are developed such that they have several compartments that fall within the range of distances in biological fibers. Also, the average translation of solutions used for the preparation of the phantoms should reflect the displacement range of water molecules.<sup>8</sup>

There have been suggestions that MRI phantoms made from agarose gel should contain concentrations of agar up to 2% (w/v).<sup>2</sup> This would ensure that the proton density and relaxation properties of these gels are within the range of human soft tissues.<sup>2</sup> As the concentration of agar in DW-MRI phantoms increases above 2%, its estimated  $T_2$  values decrease. At agar solution concentrations between 0.25 and 2% (w/v), ADC values are independent of agar concentration. For sucrose solutions, concentration levels in MRI phantoms have an influence on  $T_2$  relaxation and ADC of the solution. When the sucrose concentration is increased from 2.5 to 30% (w/w), the  $T_2$  and ADC values decrease from 250.5 to 54.6 ms and  $1.974$  to  $1.082 \times 10^{-3} \text{ mm}^2/\text{s}$ , respectively. ADC values of human soft tissues can only be attained at a sucrose solution of  $\geq 20\%$  (w/w).<sup>2</sup>

Since DWI depends on  $T_2$  relaxation times, when chemical compounds such as sucrose and agarose gel, gelatine, dairy cream, and polyethylene glycol (PEG) are added to MRI phantoms, they restrict the diffusivity of water molecules through them. This may result in a change in  $T_2$  relaxation times out of the range for soft tissues, produce mixed diffusion and affect the contrast of DW- and  $T_2$ -weighted images of the phantom. The resulting effect on image contrast may cause  $T_2$  shine-through effect, which also may influence the ADC values quantitatively. In such situations, adding gadolinium salt and gadobutrol to the contents of the phantom has been suggested as means of controlling the  $T_2$  relaxation times.<sup>23</sup>

N-tridecane has been identified to have ADC similar to that of the brain.<sup>12</sup> However, it is toxic and therefore has limited use in practice. On the other hand, solutions such as sucrose and agarose gel have ADC values close to biological tissue and are

non-toxic. However, they undergo biological degradation and therefore are not suitable for long-term scanning since they are not durable. PEG can efficiently control ADC values but has an effect on  $T_2$  relaxation time.<sup>12</sup>

Considering these identified limitations, advances in the design and construction of reference DW-MRI phantoms for quality control tests should focus on novel approaches that can compensate for the individual limitations of these materials, liquids, and solutions that make up the phantoms. Compensating for these limitations would require the development of a multifunctional substance that exhibits all the characteristics ideal for a DW-MRI phantom. It is possible to synthesize all relevant compounds from each of the individual liquids, gels, and solutions into a single substance that would compensate for the individual limitations. Because of their long-term stability and ease of manufacturing, synthetic polymer-based gels can be an excellent alternative to agar. For example, if n-tridecane is found to be stable but toxic, it is possible to synthesize the active compounds that prevent n-tridecane from undergoing biological degradation. Similarly, it is also possible to synthesize the active compound that makes agarose and sucrose gel non-toxic.

Compounds such as aqueous solutions of polyvinylpyrrolidone (PVP) could be substitutes for agarose because of their non-toxic nature and long-term stability. In the same way, active compounds that enable PEG to efficiently control ADC values could equally be isolated. So, when all these active compounds are used in the preparation of a single multifunctional substance, it is possible to have a novel phantom that would satisfy all the ideal requirements needed to perform DW imaging quality control with good reliability. Using this synthesized compound, various types of DW-MRI quality control phantoms can be made to mimic specific human tissues. **Table 3** shows a summary of some DWI phantoms in terms of ADCs achieved, stability, and  $T_2$  values.

The geometry of the phantom affects its MR image quality. For instance, a non-uniform geometry would cause a non-homogeneous magnetic field to introduce geometrical distortions in the diffusion-weighted image of the phantom. Therefore, the use of well-defined geometries such as spheres and cylinders would help reveal all possible distortions without necessarily corrupting the signal-to-noise ratio (SNR) of the image.<sup>12</sup>

**Table 3. Behavior of DWI phantoms with respect to ADC range, temperature, stability, and  $T_2$  values obtained from available literature**

Types of DWI phantom	Description of concentrations	ADC range achieved	Temp. (°C)	Stability (%CV)	$T_2$ Values (ms)	Ref.
Polysaccharide gel (TX-150) phantom	3 to 21 % TX-150 composition by weight	No ADC according to the study	5-15	No CV according to the study	57 - 287	16
Nickel chloride phantom	0.48 to 3.7 mM	No ADC according to the study	37	1.9 - 3.4	48 - 234	18
	31.8 mm/L Nickel Chloride in water	$[(2.0 \pm 0.363) \text{ to } (2.1 \pm (0.109))] \times 10^{-3} \text{ mm}^2\text{s}^{-1}$	19	No CV according to the study	No $T_2$ values according to the study	32
Ni doped agarose and sucrose	sucrose concentration 14 to 38 (% w/v), agarose concentration 0.8 to 1.2 (% w/v), nickel concentration 0.6 to 1.8 (% w/v)	$0.74 - 1.91 \times 10^{-3} \text{ mm}^2\text{s}^{-1}$	21	No CV according to the study		33
Acrylic perspex phantom (Carbomer-980)	concentration of 0.5%		37	No CV according to the study	$1453.29 \pm 13$	34
Sucrose phantom	concentration 0 to 57%	$34.9 \text{ and } 231 \times 10^{-5} \text{ mm}^2\text{s}^{-1}$	21-23	<5	No $T_2$ values according to the study	15
	0 to 1.2 M	$0.33 \text{ and } 3.02 \times 10^{-3} \text{ mm}^2\text{/sec}^{-1}$	37	No CV according to the study	No $T_2$ values according to the study	22
Polyethylene glycol (PEG) phantom	PEG concentrations from 2.5 to 20 mM	$< 1.0 \times 10^{-3} \text{ mm}^2\text{s}^{-1}$	22	1.20 - 4.62	No $T_2$ values according to the study	35
	PEG concentrations from 0 to 120 mM	$0.37 - 3.67 \times 10^{-3} \text{ mm}^2\text{s}^{-1}$	18-45	No CV according to the study	No $T_2$ values according to the study	36
Polyacrylamide gels	concentration 10% to 50% (w/v)	$(55.82 - 155.18) \times 10^{-5} \text{ mm}^2\text{s}^{-1}$	20-22	5.1	1995.8 - 110.8	37
	concentration 0% to 40% (co-monomer ratio = ¼)	$(77.3 - 231) \times 10^{-5} \text{ mm}^2\text{s}^{-1}$	21-23	≤5	No $T_2$ values according to the study	15
Agarose gel	concentration 1% to 6% (w/v)	$199.31 - 207.76 \text{ mm}^2\text{s}^{-1}$	20-22	<5	26.5 - 136.3	37
PVP	PVP-concentrations ranging from 10% (w/w) to 50% (w/w)	$1.594 - 0.3326 \mu\text{m}^2\text{/ms}$	20	No CV according to the study	No $T_2$ values according to the study	38
	PVP 15% to 65% (w/v)	average diffusivity $800 \times 10^{-12} \text{ m}^2\text{/s}$	22	2	196	39

In addition to geometrical distortion, the single-shot echo-planar imaging (SS-EPI) sequence mostly used for DWI also introduces some level of distortion in diffusion-weighted images as it is compromised by the presence of artifacts. To optimize SNR and obtain the desired ADC values, the shortest echo time and parallel imaging techniques should be applied for EPI-DWI.<sup>29</sup> Complex tissue properties such as anisotropy and perfusion should be incorporated into the design features of DWI reference phantoms in tissue compartments. Anisotropic diffusion properties should be straightforward to create, with measurable pore geometrics (e.g., water-filled glass capillary array). This could allow diffusion MRI signals to be computed based on their estimated pore morphology.<sup>30</sup> On the other hand, perfusion design and configuration can be modeled to include a variety of tissues in the overall phantom, verified and validated to cover the full physiological range.<sup>31</sup> These properties could be used to evaluate quality control diffusion parameters such as SNR, geometrical accuracy, low contrast object detectability and signal intensity uniformity.

MRI phantoms filled with paramagnetic solutions such as those containing NiCl<sub>2</sub> may not be the best choice for DWI QC

images due to their high diffusivity, unlike biological tissues. Additionally, they have  $T_1$  that is almost identical to  $T_2$ , which is not found in biological tissues.<sup>12</sup> However, NiCl<sub>2</sub> phantoms have proven to have long stability for more than 1-year period.<sup>20</sup> One major advantage of PEG and agarose is their wide range of ADC values for both free and restricted diffusion in magnetic resonance images, while sucrose can control large ADC values. As a result, NiCl<sub>2</sub> could be doped with agarose or sucrose, or PEG to accurately mimic biological tissues. The major challenge associated with the sucrose phantom is that the ADC values obtained are based on changes in free diffusion only, unlike restricted diffusion in human tissues as a result of high tissue cellularity and perfusion effect. On the other hand, phantoms made of polyacrylamide have less bacterial infiltration, and longer shelf life. Due to the utilization of cross-linking polymerization rather than a thermal gelation method, polyacrylamide phantoms may offer more mechanical strength and robustness than agarose.<sup>26</sup> Additional advantages and disadvantages of the gels and solutions used for DWI phantoms are presented in **Table 4**.

**Table 4. Advantages and disadvantages of solutions and gels used for DW phantoms**

Type of gel/solution	Advantages	Disadvantages
Agarose gel	<ul style="list-style-type: none"> <li>• non-toxic</li> <li>• ease, and low-cost fabrication</li> <li>• sufficient mechanical strength, can be formulated in different shapes and layered structures</li> <li>• ADC values are closer to biological tissue</li> <li>• excellent MR signal characteristics</li> </ul>	<ul style="list-style-type: none"> <li>• prone to bacteriological attacks</li> <li>• not suitable for long-term scanning, need high thermal treatment (80–100°C) during the preparation process</li> <li>• cooling rate and liquid temperature affect phantom homogeneity when attempting to target a particular tissue's relaxation times</li> <li>• the concentration of agarose impacts the gel's structural integrity and relaxation qualities.</li> </ul>
Polyacrylamide gels	<ul style="list-style-type: none"> <li>• excellent optical transparency</li> <li>• solid elastic and easily shaped into complex forms</li> <li>• inherent absence of air inside the gel volume, more resistant for diameters ranging from 5 to 50 μm</li> <li>• better at simulating ADC values of human tissues and human body fluids measured at ambient temperatures of 20-22°C as compared to agarose gels</li> </ul>	<ul style="list-style-type: none"> <li>• highly toxic before polymerization</li> <li>• more difficult to prepare and handle compared to agarose gels</li> <li>• new gel is needed for each experiment</li> </ul>
Sucrose solution	<ul style="list-style-type: none"> <li>• non-toxic</li> <li>• ADC values are closer to biological tissue</li> <li>• can efficiently measure and control ADC values</li> <li>• enables the simulation of <math>T_2</math> relaxation in breast tissues</li> </ul>	<ul style="list-style-type: none"> <li>• not suitable for long-term scanning</li> <li>• air in the form of air bubbles is most of the time present in sucrose solutions</li> </ul>
PEG	<ul style="list-style-type: none"> <li>• PEG decreased restricted diffusion</li> <li>• can efficiently control ADC values</li> <li>• low-cost and transparent</li> <li>• mimics a large range of ADC values for both free and restricted diffusion</li> </ul>	<ul style="list-style-type: none"> <li>• restrictions on accurately simulating restricted diffusion after a certain point since it lacks a physical restricting structure (e.g., membrane)</li> <li>• low mechanical stability</li> </ul>
Polysaccharides	<ul style="list-style-type: none"> <li>• polysaccharide materials of the CAGN phantom are not expensive and are readily available</li> <li>• strong and elastic and can be formed into a torso,</li> </ul>	<ul style="list-style-type: none"> <li>• short term preservation due to water evaporation and bacterial growth</li> </ul>
PVP	<ul style="list-style-type: none"> <li>• the ADC values of PVP at higher temperatures (like 37°C) encompass the entire spectrum of isotropic diffusion in the human body</li> <li>• reproducibility of ADC values from cancerous tumors to normal breast tissue is achievable</li> </ul>	<ul style="list-style-type: none"> <li>• <math>T_2</math> and ADC values do not cover the entire physiological range</li> </ul>
Nickel chloride solution	<ul style="list-style-type: none"> <li>• high stability</li> <li>• homogeneous</li> <li>• water-soluble</li> <li>• ease of creating phantoms with relaxation times within the range usual for biological tissue</li> </ul>	<ul style="list-style-type: none"> <li>• temporal stability</li> </ul>

## Conclusion

Optimization of DW-MRI requires routine monitoring of the performance of the MRI scanner with a standard DWI phantom. However, there is not yet a one-fits-all reference phantom and established protocol for performing diffusion-weighted imaging. The major challenge limiting the development of a reference DWI phantom is the appropriateness of solutions and/or gels used to fill the phantom. There is however the potential in synthesizing a standard multifunctional compound to fill the phantom, by utilizing the strengths of the already available gels and solutions for various DWI phantom designs.

## Recommendations

A single multifunctional tissue-mimicking substance that fills the phantom should be developed. The geometry of the vessel containing the multifunctional substance should either be spherical or cylindrical. The materials making up this substance should be easily accessible, reproducible, cost-effective, non-degradable, and non-toxic. The ADC and  $T_2$  values should cover a wide range of those of biological tissues with a coefficient of variation  $\leq 5\%$ . Multi-centre studies could be commissioned to establish DWI quality control protocols across different scanner types, if necessary, using the phantom.

## References

1. Drake-Pérez M, Boto J, Fitsiori A, Lovblad K, Vargas MI. Clinical applications of diffusion weighted imaging in neuroradiology. *Insights into Imaging*. 2018;9(4):535-47. <https://doi.org/10.1007/s13244-018-0624-3>
2. Laubach HJ, Jakob PM, Loevblad KO, et al. A phantom for diffusion-weighted imaging of acute stroke. *Journal of Magnetic Resonance Imaging*. 1998;8(6):1349-1354. <https://doi.org/10.1002/jmri.1880080627>
3. Bammer R. Basic principles of diffusion-weighted imaging. *European Journal of Radiology*. 2003;45(3):169-84. [https://doi.org/10.1016/S0720-048X\(02\)00303-0](https://doi.org/10.1016/S0720-048X(02)00303-0)
4. Tang L, Zhou XJ. Diffusion MRI of cancer: From low to high b-values. *Journal of Magnetic Resonance Imaging*. 2019;49(1):23-40. <https://doi.org/10.1002/jmri.26293>
5. Rosenkrantz AB, Padhani AR, Chenevert TL, et al. Body diffusion kurtosis imaging: basic principles, applications, and considerations for clinical practice. *Journal of Magnetic Resonance Imaging*. 2015;42(5):1190-202. <https://doi.org/10.1002/jmri.24985>
6. Granata V, Fusco R, Setola SV, et al. Diffusion kurtosis imaging and conventional diffusion weighted imaging to assess electrochemotherapy response in locally advanced pancreatic cancer. *Radiology and Oncology*. 2019;53(1):15-24. <https://doi.org/10.2478/raon-2019-0004>
7. Bennett KM, Schmainda KM, Bennett R, Rowe DB, Lu H, Hyde JS. Characterization of continuously distributed cortical water diffusion rates with a stretched-exponential model. *Magnetic Resonance in Medicine*. 2003;50(4):727-34. <https://doi.org/10.1002/mrm.10581>
8. Posnansky OP, Shah NJ. On the problem of diffusivity in heterogeneous biological materials with random structure. *Journal of Biological Physics*. 2008;34(6):551-567. <https://doi.org/10.1007/s10867-008-9119-7>
9. Cooper RL, Chang DB, Young AC, Martin CJ, Ancker-Johnson B. Restricted diffusion in biophysical systems: experiment. *Biophysical Journal*. 1974;14(3):161-177. [https://doi.org/10.1016/S0006-3495\(74\)85904-7](https://doi.org/10.1016/S0006-3495(74)85904-7)
10. Malyarenko DI, Pang Y, Amouzandeh G, Chenevert TL. Numerical DWI phantoms to optimize accuracy and precision of quantitative parametric maps for non-Gaussian diffusion. *Proc. SPIE 11313, Medical Imaging 2020: Image Processing*, 113130W. 2020. <https://doi.org/10.1117/12.2549412>
11. Kato H, Kuroda M, Yoshimura K, et al. Composition of MRI phantom equivalent to human tissues. *Medical Physics*. 2005;32(10):3199-3208. <https://doi.org/10.1118/1.2047807>
12. de Souza EM, Costa ET, Castellano G. Phantoms for diffusion-weighted imaging and diffusion tensor imaging quality control: a review and new perspectives. *Research on Biomedical Engineering*. 2017;33(2):156-165. <https://doi.org/10.1590/2446-4740.07816>
13. Kıvrak AS, Paksoy Y, Erol C, et al. Comparison of apparent diffusion coefficient values among different MRI platforms: a multicenter phantom study. *Diagn Interv Radiol*. 2013;19(6):433-437. <https://doi.org/10.5152/dir.2013.13034>
14. Hubbard PL, Zhou FL, Eichhorn SJ, Parker GJ. Biomimetic phantom for the validation of diffusion magnetic resonance imaging. *Magnetic Resonance in Medicine*. 2015;73(1):299-305. <https://doi.org/10.1002/mrm.25107>
15. Kalaitzakis G, Boursianis T, Gourzoulidis G, et al. Apparent diffusion coefficient measurements on a novel diffusion weighted MRI phantom utilizing EPI and HASTE sequences. *Physica Medica*. 2020;73:179-189. <https://doi.org/10.1016/j.ejmp.2020.04.024>
16. Groch MW, Urbon JA, Erwin WD, Al-Dooan S. An MRI tissue equivalent lesion phantom using a novel polysaccharide material. *Magnetic Resonance Imaging*. 1991;9(3):417-421. [https://doi.org/10.1016/0730-725X\(91\)90430-T](https://doi.org/10.1016/0730-725X(91)90430-T)

17. Mazzara GP, Briggs RW, Wu Z, Steinbach BG. Use of a modified polysaccharide gel in developing a realistic breast phantom for MRI. *Magnetic Resonance Imaging*. 1996;14(6):639-648. [https://doi.org/10.1016/0730-725X\(96\)00054-9](https://doi.org/10.1016/0730-725X(96)00054-9)
18. Vassiliou VS, Heng EL, Gatehouse PD, et al. Magnetic resonance imaging phantoms for quality-control of myocardial T1 and ECV mapping: specific formulation, long-term stability and variation with heart rate and temperature. *Journal of Cardiovascular Magnetic Resonance*. 2016;18(1):1-12. <https://doi.org/10.1186/s12968-016-0275-9>
19. Lavdas I, Behan KC, Papadaki A, McRobbie DW, Aboagye EO. A phantom for diffusion-weighted MRI (DW-MRI). *Journal of Magnetic Resonance Imaging*, 2013;38(1):173-179. <https://doi.org/10.1002/jmri.23950>
20. Captur G, Gatehouse P, Keenan KE, et al. A medical device-grade T1 and ECV phantom for global T1 mapping quality assurance—the T1 Mapping and ECV Standardization in cardiovascular magnetic resonance (TIMES) program. *Journal of Cardiovascular Magnetic Resonance*. 2016;18(1):1-20. <https://doi.org/10.1186/s12968-016-0280-z>
21. Kim JH, Kim JH, Lee SH., Park J, Lee SK. Fabrication of a spherical inclusion phantom for validation of magnetic resonance-based magnetic susceptibility imaging. *PLOS One*. 2019;14(8):e0220639. <https://doi.org/10.1371/journal.pone.0220639>
22. Hara M, Kuroda M, Ohmura Y, et al. A new phantom and empirical formula for apparent diffusion coefficient measurement by a 3 Tesla magnetic resonance imaging scanner. *Oncology Letters*. 2014;8(2):819-824. <https://doi.org/10.3892/ol.2014.2187>
23. Gatidis S, Schmidt H, Martirosian P, Schwenzer NF. Development of an MRI phantom for diffusion-weighted imaging with independent adjustment of apparent diffusion coefficient values and T2 relaxation times. *Magnetic Resonance in Medicine*. 2014;72(2):459-463. <https://doi.org/10.1002/mrm.24944>
24. Le Bihan D, Iima M. Diffusion magnetic resonance imaging: what water tells us about biological tissues. *PLOS Biology*. 2015;13(7):e1002203. <https://doi.org/10.1371/journal.pbio.1002246>
25. Khasawneh A, Kuroda M, Yoshimura Y, et al. Development of a novel phantom using polyethylene glycol for the visualization of restricted diffusion in diffusion kurtosis imaging and apparent diffusion coefficient subtraction method. *Biomedical Reports*. 2020;13:52. <https://doi.org/10.3892/br.2020.1359>
26. Hariri A, Palma-Chavez J, Wear KA, Pfefer TJ, Jokerst JV, Vogt WC. Polyacrylamide hydrogel phantoms for performance evaluation of multispectral photoacoustic imaging systems. *Photoacoustics*. 2021;22:100245. <https://doi.org/10.1016/j.pacs.2021.100245>
27. Stringer R. Electrophoresis overview. *Encyclopedia of Analytical Science (Second Edition)*, Elsevier 2005, Pages 356-363, <https://doi.org/10.1016/B0-12-369397-7/00120-5>
28. Fieremans E, Lee HH. Physical and numerical phantoms for the validation of brain microstructural MRI: A cookbook. *Neuroimage*. 2018;182:39-61. <https://doi.org/10.1016/j.neuroimage.2018.06.046>
29. Yoshida T, Urikura A, Shirata K, Nakaya Y, Terashima S, Hosokawa Y. Image quality assessment of single-shot turbo spin echo diffusion-weighted imaging with parallel imaging technique: a phantom study. *The British Journal of Radiology*. 2016;89(1065):20160512. <https://doi.org/10.1259/bjr.20160512>
30. Komlosh ME, Benjamini D, Barnett AS, et al. Anisotropic phantom to calibrate high-q diffusion MRI methods. *Journal of Magnetic Resonance*. 2017;275:19-28. <https://doi.org/10.1016/j.jmr.2016.11.017>
31. Kamphuis ME, Greuter MJ, Slart RH, Slump CH. Quantitative imaging: systematic review of perfusion/flow phantoms. *European Radiology Experimental*. 2020;4(1):1-13. <https://doi.org/10.1186/s41747-019-0133-2>
32. Al-Mulla M, McGee A, Kenny P, Rainford L. Quality Assurance Phantom Testing of an Echo-Planar Diffusion-Weighted Sequence on a 3T Scanner. *Adv Res Foot Ankle: ARFA-110*. 2019;11.
33. Shurche S, Riahi N. Diffusion Phantom Assessment in 3 Tesla MRI Scanner. *Frontiers in Biomedical Technologies*. 2016;3(1-2):34-40.
34. Hellerbach A, Schuster V, Jansen A, Sommer J. MRI phantoms—are there alternatives to agar? *PloS One*. 2013;8(8):e70343. <https://doi.org/10.1371/journal.pone.0070343>
35. Sato E, Fukuzawa K, Takashima H, et al. Evaluation of a Polyethylene Glycol Phantom for Measuring Apparent Diffusion Coefficients Using Three 3.0 T MRI Systems. *Applied Magnetic Resonance*. 2021;52(5):619-31. <https://doi.org/10.1007/s00723-021-01336-z>
36. Matsuya R, Kuroda M, Matsumoto Y, et al. A new phantom using polyethylene glycol as an apparent diffusion coefficient standard for MR imaging. *International Journal of Oncology*. 2009;35(4):893-900. [https://doi.org/10.3892/ijo\\_00000404](https://doi.org/10.3892/ijo_00000404)
37. Boursianis T, Kalaitzakis G, Pappas E, Karantanas AH, Maris TG. MRI diffusion phantoms: ADC and relaxometric measurement comparisons between polyacrylamide and agarose gels. *European Journal of Radiology*. 2021;139:109696. <https://doi.org/10.1016/j.ejrad.2021.109696>
38. Wagner F, Laun FB, Kuder TA, et al. Temperature and concentration calibration of aqueous polyvinylpyrrolidone (PVP) solutions for isotropic diffusion MRI phantoms. *PloS One*. 2017;12(6):e0179276. <https://doi.org/10.1371/journal.pone.0179276>
39. Pierpaoli C, Sarlls J, Nevo U, Basser PJ, Horkay F. Polyvinylpyrrolidone (PVP) water solutions as isotropic phantoms for diffusion MRI studies. *Proc Intl Soc Magn Reson Med*. 2009;17:1414.